Modeling suggests SARS-CoV-2 rebound after nirmatrelvir-ritonavir treatment is driven by target cell preservation coupled with incomplete viral clearance

Tin Phan[1], Ruy M. Ribeiro[1], Gregory E. Edelstein[2], Julie Boucau[3], Rockib Uddin[4], Caitlin Marino[3], May Y. Liew[4], Mamadou Barry[4], Manish C. Choudhary[2], Dessie Tien[4], Karry Su[4], Zahra Reynolds[4], Yijia Li[2,4,5], Shruti Sagar[4], Tammy D. Vyas[4], Yumeko Kawano[2], Jeffrey A. Sparks[2], Sarah P. Hammond[4], Zachary Wallace[4], Jatin M. Vyas[4], Jonathan Z. Li[2†], Mark J. Siedner[4,7†], Amy K. Barczak[3,4†], Jacob E. Lemieux[4,6†], and Alan S. Perelson[1,8]*.

Affiliations:

[1]Theoretical Biology and Biophysics Group, Los Alamos National Laboratory, Los Alamos, NM 87544, USA.

[2]Department of Medicine, Brigham and Women's Hospital, Harvard Medical School, Boston, MA 02115, USA

[3]Ragon Institute of MGH, MIT and Harvard, Cambridge, MA 02139, USA

[4]Department of Medicine, Massachusetts General Hospital, Havard Medical School, Boston, MA 02114, USA

[5]University of Pittsburgh Medical Center, Pittsburgh, PA 15261, USA

[6]Broad Institute, Cambridge, MA 02142, USA

[7]Africa Health Research Institute, KwaZulu-Natal, South Africa

[8]Santa Fe Institute, Santa Fe, NM 87501, USA

[†]Equal contributions

*Corresponding author.

Email: asp@lanl.gov (ASP)

Abstract: In a subset of SARS-CoV-2 infected individuals treated with the oral antiviral nirmatrelvir-ritonavir, the virus rebounds following treatment. The mechanisms driving this rebound are not well understood. We used a mathematical model to describe the longitudinal viral load dynamics of 51 individuals treated with nirmatrelvir-ritonavir, 20 of whom rebounded. Target cell preservation, either by a robust innate immune response or initiation of nirmatrelvir-ritonavir near the time of symptom onset, coupled with incomplete viral clearance, appear to be the main factors leading to viral rebound. Moreover, the occurrence of viral rebound is likely influenced by time of treatment initiation relative to the progression of the infection, with earlier treatments leading to a higher chance of rebound. Finally, our model demonstrates that extending the course of nirmatrelvir-ritonavir treatment, in particular to a 10-day regimen, may greatly diminish the risk for rebound in people with mild-to-moderate COVID-19 and who are at high risk of progression to severe disease. Altogether, our results suggest that in some individuals, a standard 5-day course of nirmatrelvir-ritonavir starting around the time of symptom onset may not completely eliminate the virus. Thus, after treatment ends, the virus can rebound if an effective adaptive immune response has not fully developed. These findings on the role of target cell preservation and incomplete viral clearance also offer a possible explanation for viral rebounds following other antiviral treatments for SARS-CoV-2.

Importance:

Nirmatrelvir-ritonavir is an effective treatment for SARS-CoV-2. In a subset of individuals treated with nirmatrelvir-ritonavir, the initial reduction in viral load is followed by viral rebound once treatment is stopped. We show the timing of treatment initiation with nirmatrelvir-ritonavir may influence the risk of viral rebound. Nirmatrelvir-ritonavir stops viral growth and preserves

target cells but may not lead to full clearance of the virus. Thus, once treatment ends, if an effective adaptive immune response has not adequately developed, the remaining virus can lead to rebound. Our results provide insights into the mechanisms of rebound and can help develop better treatment strategies to minimize this possibility.

Introduction

A 5-day course of nirmatrelvir-ritonavir (N-R) is recommended for individuals who test positive for SARS-CoV-2 with mild-to-moderate symptoms and a high risk of progression to severe disease [1]. Treatment with two doses (300 mg of nirmatrelvir and 100 mg of ritonavir) per day is suggested to be initiated as soon as possible and within 5 days of symptom onset. Nirmatrelvir is a protease inhibitor, targeting the SARS-CoV-2 main protease 3-chymotrypsin–like cysteine protease enzyme (3CLpro), blocking SARS-CoV-2 replication. Ritonavir reduces the liver catabolism of nirmatrelvir and thus prolongs the half-life of nirmatrelvir [1]. While N-R substantially reduces the risk of progression to severe COVID-19 and can shorten the duration of disease in high-risk individuals [2–4], in some cases, viral rebound and recurring symptoms occur after the 5-day treatment course, including in individuals who have been vaccinated and/or boosted [5,6]. Some individuals with viral rebound are reported to have culturable virus up to 16 days after the initial diagnosis [6,7], thus, potential transmission to close contacts during the rebound period is a concern [5]. Although virus resistant to N-R *in vitro* [8,9] and treatment-emergent 3CLpro substitutions *in vivo* [1,10] have been observed, viral rebound in the case of N-R *in vivo* does not seem to be caused by the emergence of drug resistant mutants [5–7,11–14]. However, two immunocompromised individuals, who were treated with extended duration of N-R in combinations with other treatments, experienced viral rebound associated with resistant mutations E166 A/V and L50F in the NSP5 region where 3CLpro is located [15,16].

The precise proportion of individuals treated with N-R that exhibit viral rebound is unclear, and estimates could vary based on a range of factors, including the definition used to classify rebound and viral characteristics. For example, in the N-R phase 3 clinical trial, EPIC-HR, the fraction of individuals with viral rebound (positive PCR test) and recurring symptom

was 1-2% [17]. However, this study was limited by the relatively infrequent viral RNA measurements after the completion of N-R. Other studies have reported rebound in 0.8 – 27% of N-R treated individuals [6,18–22]. Viral rebound has also been described in untreated individuals [23,24], but often at a lower frequency compared to N-R treated individuals regardless of rebound definition [6,17,19,20,22,25,26].

Previously, we analyzed the data presented in Charness et al. [5], where quantitative PCR is available for three individuals who experienced viral and symptom rebound after taking N-R. In all three individuals, no resistance mutations in the gene encoding the protease targeted by nirmatrelvir (3CLpro) developed during treatment and there was no evidence of reinfection by a different variant. The viral dynamic models in our study adequately captured the viral rebound dynamics in all three individuals [27]. One hypothesis we tested was that a 5-day N-R treatment course started near the time of symptom onset reduces the depletion of target cells but does not fully eliminate the virus, thus allowing the virus to rebound once treatment is stopped. The occurrence of viral rebound was shown to be sensitive to model parameters, especially the time therapy is started and the time adaptive immune response begins to emerge. This suggested that a delay in the treatment initiation can lower the chance of rebound. However, our results were only supported by a limited data set comprised of three individuals [27].

Here, we expand upon this previous study using data from an ongoing observational cohort study, including 51 individuals treated with N-R, 20 of whom were classified as having viral rebound per the definition by Edelstein et al. [6] (additional details in Data). Our model accurately captured the viral dynamics of all 51 individuals and provides further evidence that target cell preservation plays a central role in the occurrence of large amplitude viral rebounds. Our model predicts that target cell preservation was achieved by a robust innate immune

response or by early treatment. As treatment only stops viral replication but does not directly eliminate existing virus, residual virus may remain after treatment has ended and can infect the remaining target cells and rebound. While we use N-R as a case study, our theory can also explain the viral rebound observed after treatment with molnupiravir [21], another oral antiviral with FDA emergency use authorization, simnotrelvir/ritonavir [28], a protease inhibitor that also targets the SARS-CoV-2 main protease 3CLpro but has a shorter half-life [29] than nirmatrelvir, and VV116 or mindeudesivir [30], an inhibitor of the viral RNA-dependent RNA polymerase that is not inferior to N-R in reducing time to recovery [31].

Results

Model of viral dynamics in the upper respiratory tract

We used an extension of a viral dynamic model that has been applied to study SARS-CoV-2 infection dynamics [32–35]. In this model (depicted in Fig 1), viral infection of target cells in the upper respiratory tract (URT) occurs with rate constant β. After spending an average time of $1/k$ in an eclipse phase E, infected cells enter a productively infected state I, where they produce virus at rate p (in the absence of N-R) and die at per capita rate δ. SARS-CoV-2 is cleared at per capita rate c.

For the innate immune response, we assumed the amount of type-I and type-III interferons in the URT is proportional to the number of infected cells, I, and that interferon puts target cells into a temporary antiviral state (refractory to infection) [33,34,36–39] at rate ϕ. Refractory cells become susceptible to infection again at rate $\rho(I) = \rho\frac{K_\rho}{I+K_\rho}$, where ρ is the maximum rate at which refractory cells return to being susceptible [40] and K_ρ denotes the

density of infected cells at which the rate of return is half-maximal[1]. Following Pawelek et al. [41], the adaptive immune response is modeled as causing an exponential increase of the death rate of infected cells (δ) at rate σ for a short time after its emergence time t^*. This choice was motivated by the observation that virus-specific $CD8^+$ T cells expand exponentially after viral infection [42]. This makes the death rate of infected cells a function of time $\delta(t)$. Finally, the concentration-dependent action of N-R is incorporated using a pharmacokinetic-pharmacodynamic (PK-PD) model. Additional details of the model formulation are provided in the Methods, S1 Text, and S1 Fig.

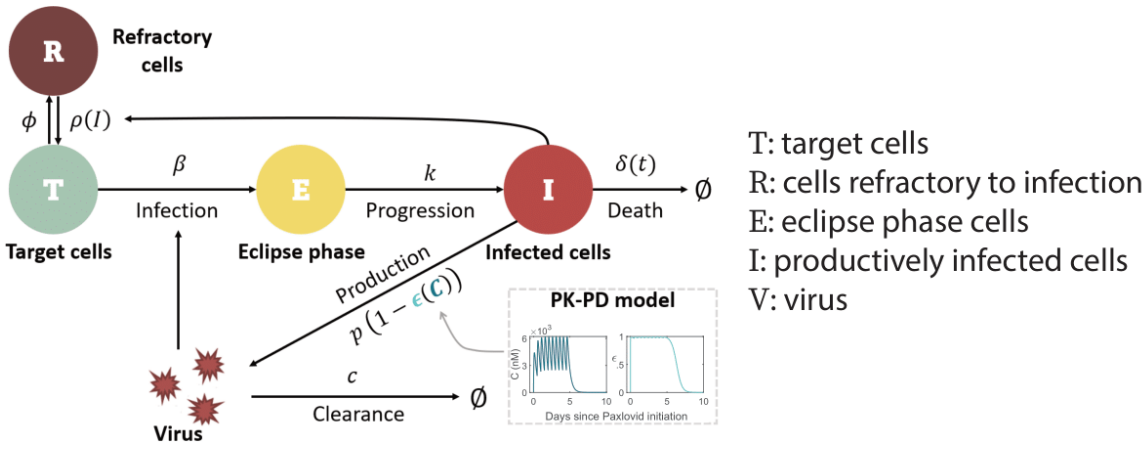

Fig 1. Schematic of the viral dynamic model. The model includes pharmacokinetic (PK) and pharmacodynamic (PD) sub-models, specifying how the drug concentration C and drug effectiveness $\epsilon(C)$ change over time (model details in Methods and S1 Text).

[1] Note if $I \gg K_\rho$, i.e. if the amount of interferon is very high, $\rho(I) \to 0$, and cells remain in an antiviral state. However, as infection resolves and I becomes much less than K_ρ, the antiviral state is lost at rate close to ρ.

Model describes the viral dynamics in all treated individuals.

Our viral dynamic model describes the observed data for treated participants with and without rebound (Fig 2a). By fitting the model to the data, we obtain population (S1 Table in S2 Text) and individual (S2 Table in S2 Text) estimates of the model parameters, which are stratified by rebound vs. non-rebound (Fig 2b). The estimated time of infection relative to the time of symptom onset as reported by participants and the time of N-R initiation relative to infection and to symptom onset are also shown in Fig 2b. We found that the parameters (ρ, ϕ, K_ρ) governing the dynamics of refractory cells, i.e., those cells that are protected from infection, are significantly different between individuals who rebound and those who do not. The differences in all of these parameters between the two groups were such that they favored the maintenance of cells in the refractory state in non-rebounders, who had a larger rate of cell entry into refractoriness ϕ (p=0.0004), a smaller maximum rate of cells returning to target status ρ (p=0.0047), and a smaller half-saturation constant for this process K_ρ (p=0.0056).

In addition, the baseline infected cell death rate (δ_0) was also significantly smaller in non-rebounders (p=0.0027). When we tested using "rebounder" as a covariate on each parameter to improve the model fit and to better understand factors distinguishing rebounders from non-rebounders, a covariate in δ_0 provided the lowest BICc. However, the BICc difference was small (less than 4 points) compared to the model without a covariate (S3 Table in S3 Text). Additionally, when we considered a variation of our best fit model with proliferation of target cells (details and model fit in S2a Fig in S4 Text), the baseline infected cell death rate was not significantly different between rebounders and non-rebounders (S2b Fig). On the other hand, there were still differences that are significant in the innate immune response parameters ϕ (p=0.0222) and K_ρ (p=0.0201). Specifically, in both models, the rebounders tend to have a larger

value of ϕ, indicating a more rapid loss of target cells by going into the refractory state initially, and a larger value of K_ρ, resulting in an earlier replenishment of target cells that can support viral rebound [43].

The time of N-R treatment relative to the estimated time of infection was about one day shorter in participants who rebounded vs. those who did not (median 3.75 days vs. 4.72 days, p=0.0003). This is consistent with the significant difference (p=0.0009) in the time of N-R initiation relative to the time of symptom onset in rebound vs. non-rebound individuals, as suggested before [6,27,43,44]. These differences in parameter estimates manifest in clear distinctions in model dynamics (viral load, target cells, infected cells) between rebounders and non-rebounders, as discussed and demonstrated in S3-4 Figs and S5 Text. A model variation that includes logistic proliferation of target cells discussed in S4 Text also predicts similar model dynamics (S5 Fig in S5 Text).

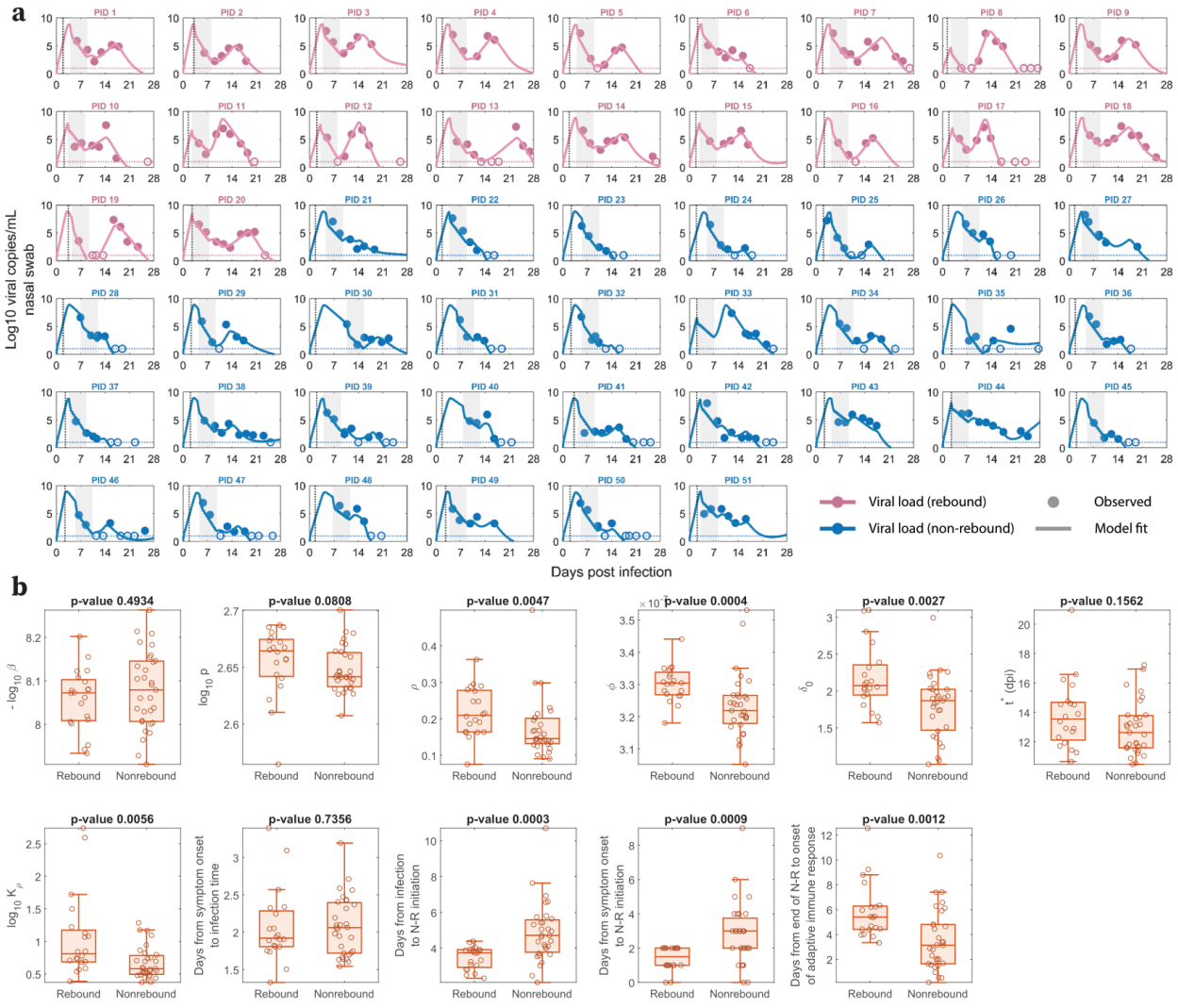

Fig 2. Model fits recapitulate viral dynamics and quantify differences in the characteristics between viral rebound and non-rebound individuals. a. Model fits to nasal viral loads of rebound (pink) and non-rebound (blue) individuals. The shaded area is the duration of N-R treatment. The dotted horizontal line is the limit of detection (LoD) for the RT-qPCR assay. Filled and open circles are data above and below the LoD, respectively. The dotted black vertical line indicates the reported time of symptom onset relative to the estimated time of infection. **b.** Box plots of best fit parameters and timing of N-R stratified by individuals who rebound vs. those who do not. The lower and upper limits of the box represent the first and third quartile,

178 respectively. The line inside the box is the median and the whiskers connect the top/bottom of
179 the box to the max/min values that are not outliers (data points further than 1.5 times the
180 interquartile range). Overlaid circles are individual parameter values. Time of N-R initiation
181 relative to symptom onset was recorded for each individual (except non-rebounder PID 23,
182 whose symptom onset is imputed at one day prior to their first positive test). P-values are
183 calculated using the Mann-Whitney U test.

184

185 The model also recapitulates the data in untreated individuals from the same ongoing
186 clinical cohort (S6a Fig in S6 Text). We also find that the parameter distribution between the
187 treated and untreated groups are statistically similar (S6b Fig in S6 Text). The one exception is
188 the average difference of 1.23 days (95% confidence interval [0.44, 2.03], p=0.0026) in the
189 estimated onset time of the adaptive immune response, which is later in treated individuals
190 compared to untreated individuals.

191

192 **The sensitivity of viral rebound to treatment initiation time and the duration of treatment.**

193 Our results suggest that the time of N-R treatment initiation and the availability of target
194 cells at that time are critical to define whether a rebound occurs or not. To further explore this,
195 we used simulation experiments to show that delaying or extending the period of treatment with
196 N-R can decrease the probability of rebound. We simulated n=20 treatment cohorts, each with
197 100 randomly generated *in silico* individuals treated with N-R (see Methods for details), and
198 assessed what percentage of individuals in each cohort exhibited rebound, defined as the viral
199 load returning above 10^4 RNA copies per mL [6]. Samples of the simulated viral dynamics for

individuals in the *in silico* cohorts are presented in S7a-c Fig in S8 Text. Without treatment, our cohorts of *in silico* individuals have similar rebound statistics as those reported in the 8 clinical studies [6,17,19,20,23–26] (S7d Fig in S8 Text).

We tested treatment starting at days 1, 2, 3 and 4 post symptom onset, with symptom onset assumed to be 3 days post infection. Extending treatment could be a feasible method of preventing rebound [27,43,45], so we also examined a 5-, 6-, 7-, 8- and 10-day treatment courses. In one scenario, we assume N-R does not affect the development of adaptive immune response (Fig 3). In a second scenario, we assume that the onset of the adaptive immune response is delayed more with longer treatments (S8 Fig in S9 Text). It is important to examine this possibility as it would make rebound more likely. The time of symptom onset is fixed at 3 days post infection; however, assuming either 2 or 4 days does not change the general trend observed in Fig 3 and S8 Fig in S9 Text in which we observed a clear decrease in rebound percentage as treatment is initiated later. We also found that an increase in the duration of treatment with N-R tends to prevent viral rebound. In all scenarios, extending treatment to 10 days decreases the probability of rebound in our 20 simulated 100-person cohorts to a level so low that it does not occur for all practical purposes.

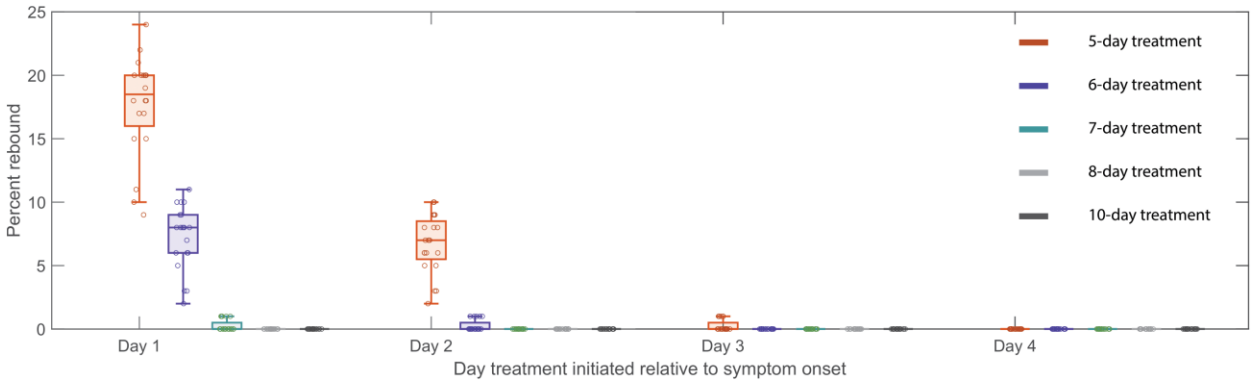

Fig 3. Predicted rebound relative to the time and duration of treatment. Predicted rebound relative to 5-, 6-, 7-, 8-, and 10-day course of N-R. Symptom onset is assumed to occur three days post infection. Boxplots depict the percentage of rebound cases from 20 *in silico* cohorts, each with 100 individuals, for different treatment initiation times. Each open circle represents the rebound percentage from one cohort. The extended duration of N-R (beyond a 5-day treatment course) is assumed to not cause additional delay on the onset of adaptive immune response.

Discussion

Here, we extended a viral dynamic model of SARS-CoV-2 infection to show that the main driver of viral rebound in the setting of treatment is the preservation of target cells, often as a result of a robust innate immune response, or early treatment initiation. Our model shows that once N-R treatment is completed and the drug is washed out before an adaptive immune response develops, residual viable viruses can rebound if there are sufficient target cells remaining. Our results support our hypothesis [27] and echo the findings of recently published modeling studies [43,46]. However, our conclusions are supported by a more robust dataset of individuals treated with N-R, considerations of alternative models and assumptions on the impact of N-R on the development of an adaptive immune response with a detailed PK-PD model.

Our best model is able to capture the viral dynamics observed in all participants. It suggests that the protective effects of innate immunity preserved the majority of target cells by putting them into an antiviral state shortly after the virus starts growing exponentially (S3-4 Figs in S5 Text). During treatment, the viral load and the number of infected cells rapidly decline (Fig 2a and S4c, f Figs in S5 Text) due to infected cell death and continuous viral clearance, concurrent with reduced viral production due to drug activity. This decline leads to a decrease in

the interferon response, causing cells to exit more quickly from the refractory state [36–40]. It is clear from the data of both rebound and non-rebound individuals that a five-day course of N-R is likely to be insufficient to completely eliminate the virus. Indeed, there was measurable virus (viral load > LoD) after the completion of treatment (the first data point after treatment) in 40 of the 51 participants (Fig 2a). Thus, if viable viruses remain after the drug is washed out and before an adaptive immune response can be mounted, virus can rebound. However, whether the virus rebounds to an observable level is also determined by the time between the end of treatment and the generation of an effective adaptive immune response, and to some degree, the differences in the maintenance of the cell refractory status (Fig 2b). This conclusion is supported by the observation that the time between the end of treatment and the predicted onset time of an adaptive immune response in the model is statistically different between the rebound and non-rebound groups. For the rebound group, the estimated time [min, max] is 5.87 [3.34, 12.56] days, and for the non-rebound group, it is 3.53 [0.14, 10.35] days ($p = 0.0012$) (Fig 2b). Note that this difference is not driven by the fitted onset time of the adaptive immune response t^* measured from the estimated time of infection, whose distribution is statistically similar between the two groups (Fig 2b). Instead, the difference in the time between the end of treatment and the onset time of the adaptive immune response is mainly driven by the earlier time of treatment initiation in the rebound group (Fig 2b).

The time of treatment initiation also plays a crucial role in determining if a rebound is observed or not. If treatment is initiated early after infection, before a time we denote $t_{critical}$, a substantial number of target cells remain unprotected after the 5-day treatment and viral rebound is likely to occur. After $t_{critical}$, too few target cells remain available to support viral growth; however, target cells still return from the refractory state as the virus is eliminated. Since viral

growth switches to viral decay at the time of the viral peak in an untreated individual, this means $t_{critical}$ is the time the viral peak is reached. In more technical terms $t_{critical}$ corresponds to the time the effective reproductive number $\Re$ equals 1, so that on average, each infected cell produces one new infected cell, leading to neither growth nor decay in the number of infected cells. In several observational/retrospective studies focusing on Omicron subvariants, the time to the viral peak is suggested to be 2 to 5 days post symptom onset [47–49]. We observed that for the participants in this study, who were all infected with Omicron subvariants, rebound is associated with treatment initiated within 2 days of symptom onset [6]. This suggests treatment might have been initiated prior to $t_{critical}$ while the virus level is still expanding. Delaying treatment may be a strategy to reduce the possibility of viral rebound (Fig 3 and S8 Fig in S9 Text); however, delaying treatment could have a negative impact on the severity of disease in the high-risk individuals for whom N-R is recommended, and this question deserves more study [50]. In addition, N-R treatment accelerates viral clearance and hence potentially can reduce viral transmission. See Fig 4 for a summary description of our results.

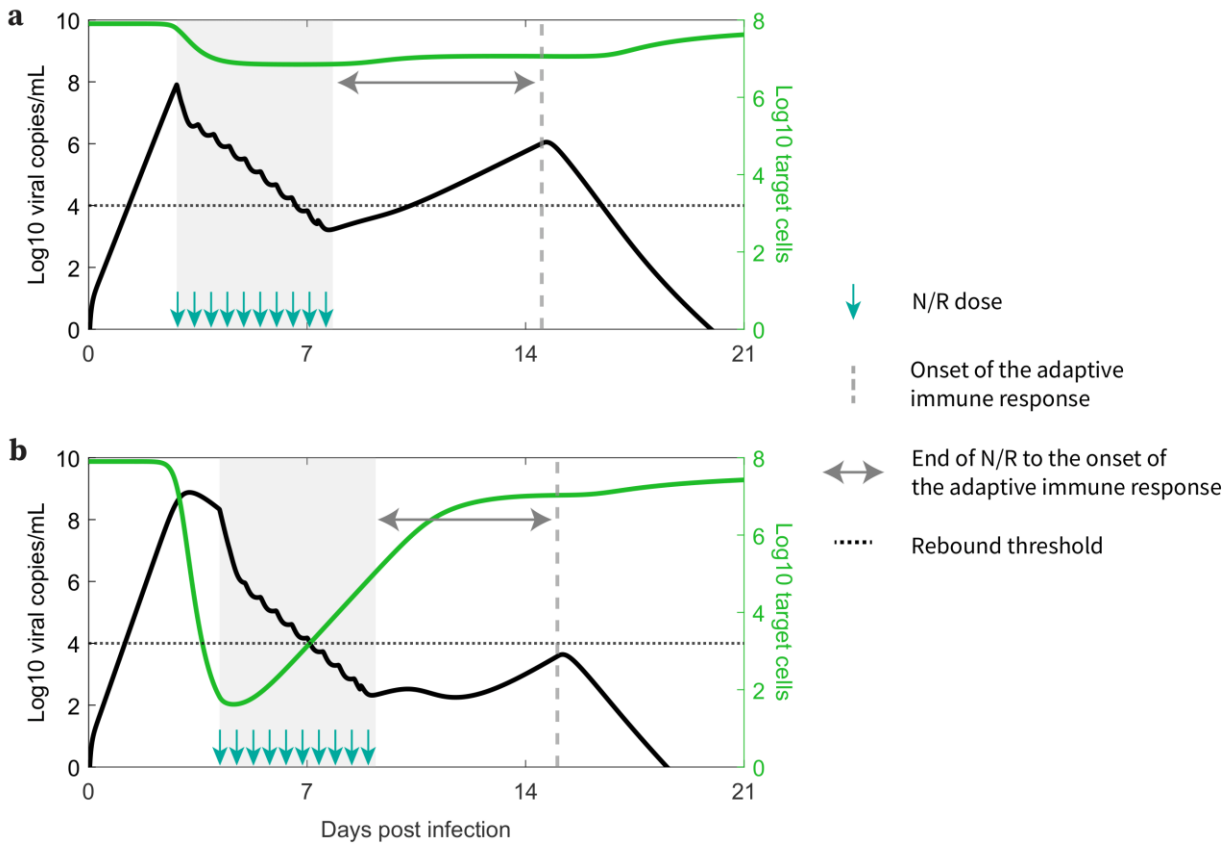

Fig 4. How early treatment correlates with higher rebound probability. **a.** Early treatments preserve more target cells and result in a longer duration between the end of N-R and the onset of an adaptive immune response, leading to a higher probability of an individual being classified as experiencing rebound. **b.** Later treatments preserve fewer target cells and result in a shorter duration between the end of N-R and the onset of an adaptive immune response, leading to a lower probability of an individual being classified as experiencing rebound.

Interestingly, all individuals studied here were vaccinated and boosted, and nonetheless had breakthrough infections with Omicron sub-variants [6]. Thus, while adaptive B and T cell immune responses did not prevent infection, they might have been present at the time of infection and could have affected the level of preserved target cells. The timing of the adaptive immune response and its expansion may play a crucial role in the occurrence of viral rebound. In

particular, without a strong adaptive immune response, even a longer course of N-R still resulted in viral rebound in immunocompromised patients with severe disease [15,16,51]. Delaying the initiation of N-R may also provide more time for the priming of the adaptive immune response and shorten the time between the end of treatment and the emergence of the adaptive immune response, which would reduce the chance of rebound.

Our model predicted that the 20 rebound participants in the studied set have both innate and adaptive immune responses comparable to those of non-rebound participants (Fig 2b). This intriguing finding is supported by the clinical observations that most viral rebounds quickly resolve within several days [52] and this correlates with a strong antibody and T-cell immune response [13]. There is also contradictory evidence suggesting that N-R may delay the development of the adaptive immune response [53,54]. We found an average of 1.23 day delay in the estimated onset time of the adaptive immune response in the treated vs. untreated groups (S6 Text). Even so, the rebound participants quickly cleared the rebounding virus. This suggests that while early initiation of N-R may slightly delay the onset of the adaptive immune response, perhaps due to lower level of antigens, it does not stop the development of an adaptive immune response in non-immunocompromised individuals. Thus, if the adaptive immune response is not significantly impeded by treatment, prolonging treatment can be beneficial in reducing rebound and does not have the possible detrimental effects on disease severity or increase viral transmission of delaying treatment [44]. Indeed, using an *in silico* cohort we show that even a modest extension to a 6-day treatment course can significantly reduce viral rebound incidence (Fig 3 and S8 Fig in S9 Text). Extensions beyond a 6-day treatment course can further reduce rebound incidence with a 10-day treatment course almost totally eliminating the possibility of rebound in our *in silico* patient cohorts (Fig 3 and S8 Fig in S9 Text). A recent clinical trial

compared 5 vs. 10 vs. 15 days treatment with N-R given to immunocompromised patients with COVID-19 (ClinicalTrials.gov: NCT05438602). The final analysis of 150 participants showed that extending treatment to 10 or 15 days can minimize the risk of rebound [55]. While 9 of 52 participants treated with 5 days of N-R rebounded, only 1 participant rebounded in the 10-day (n=48) and 15-day (n=50) treatment groups. While the clinical trial was carried out with immunocompromised patients, the single rebound incidence in the 10-day treated group supports our simulation results for a theoretical 10-day treatment for mild-to-moderate individuals with high risk of progression (Fig 3). When the cost of the drug is accounted for, the optimal treatment duration to minimize rebound and cost falls between 7 and 8 days (S9 Fig in S10 Text). However, because N-R is packaged as a 5-day course of treatment, extending treatment to 10 or 15 days may be more practical. Additionally, we previously suggested that the success of a second course of N-R once viral rebound occurs will also depend on the timing of an effective adaptive immune response in a similar manner [27]. This is corroborated by observations of recurring viral rebounds in an immunocompromised individual at the end of each treatment period, which eventually leads to the development of the resistance mutation E166V/L50F [15]. An ongoing clinical trial aims to investigate this possibility (ClinicalTrials.gov: NCT05567952).

Rather than extend treatment duration, the use of a drug with a longer half-life may be helpful, especially if infectious forms of SARS-CoV-2 can persist during antiviral treatment [8,9,56]. An ongoing clinical trial of ensitrelvir (ClinicalTrials.gov: NCT05305547) [57], a protease inhibitor that also targets SARS-CoV-2 3CLpro but with a longer half-life than nirmatrelvir [58], yielded results suggesting that this new drug was virologically active and did not significantly increase the risk of viral rebound [45].

The phenomenon of viral rebound has also been observed for monoclonal antibody treatments for SARS-CoV-2 [59–63]. One example is bamlanivimab, the first monoclonal antibody that received FDA emergency use authorization for the treatment of COVID-19 [61–63]. However, rebounds in the case of monoclonal antibodies are associated with the emergence of resistance mutations [59–63], which contrasts with the lack of evidence for resistant mutants *in vivo* in the majority of cases for the current antiviral treatments [5–7,11–13]. Yet, the emergence of resistance mutations to monoclonal antibodies does not always lead to viral rebound [59,60], suggesting other mechanisms beside selection pressure due to treatment may contribute to observable viral rebounds. Our previous modeling studies suggested that target cell regeneration mechanisms, such as homeostatic proliferation of epithelial cells [64–66] or refractory cells returning to a susceptible state, are necessary to explain the high amplitude viral rebounds observed in bamlanivimab treated participants [32]. Here our model with logistic proliferation (S4 Text) also recapitulates the viral load dynamics in rebound and non-rebound participants (S2a Fig in S4 Text) and the stratified parameter values also support the conclusion that early N-R initiations correlate with a higher probability of rebound (S2b Fig in S4 Text). However, the net regeneration effect of target cells is similar to that in the innate immune response model (S5 Fig compared to S3 Fig in S5 Text). This is likely because potent target cell preservation limits the proliferation rate, which is related to the number of cells that are lost by infection. Moreover, because rebound occurs within days after the end of treatment, there is also not sufficient time for the proliferation effect to be more evident. In addition to explaining viral rebound, target cell regeneration mechanisms may also explain the observations of low amplitude viral rebounds/persistence in untreated individuals prior to the development of an effective adaptive immune response [67,68].

Our study has some limitations, the principal of which is not knowing the precise date of infection of each individual. This is a very common situation when dealing with infectious diseases [69,70], and it is ameliorated by using a well-established dynamical model, which in most cases allows us to infer the time of infection better than may be known clinically. Another important issue is that we do not have data on the immune response, even though we include both innate and acquired immune factors in our model. In the context of vaccinated individuals, this could be even more important, although it has been shown before that the viral dynamics of breakthrough infections maybe similar to that in unvaccinated individuals [71,72]. Our study could be strengthened and validated by incorporating detailed longitudinal immune response data, similar to those collected in the human challenge study for SARS-CoV-2 [73]. Furthermore, for the logistical proliferation model, markers of target cell proliferation or re-population could be used to support the model. We should also re-emphasize that although delaying treatment leads to lower probability of rebound, we do not evaluate the effect on severity of disease.

In summary, our results suggest the occurrence of viral rebound following a complete course of N-R may be due to the level of preserved target cells in the setting of incomplete elimination of the virus. Delaying initiation of treatment for a day or a few days following the first signs of infection should have some benefit in reducing the possibility of rebound, but at the cost of allowing viral growth to continue and the possibility of increased disease severity. On the other hand, extending treatments by several days may also reduce the likelihood of rebound, but at an increased cost of drug. We remark that viral rebound is not an intrinsic feature of our model, but rather a possibility within the model dynamical landscape. This is clearly demonstrated by the model fits to non-rebound individuals (treated and untreated). Lastly,

rebound following antiviral treatments is not unique to N-R [21,28]. In particular, rebound without evidence of resistance has also been observed for the protease inhibitor simnotrelvir [28], which has a similar mechanism of action to nirmatrelvir and a shorter half-life [29]. Thus, these findings may provide an explanation for rebound following other antiviral treatments besides N-R.

Methods

Data

The data in this study comes from an ongoing observational cohort study. Full details of the study design and observations have been reported previously [6]. In summary, participants are adult outpatients selected from those who took part in the POSITIVES study (Post-vaccination Viral Characteristics Study) [7,74] within 5 days of an initial positive diagnostic test for COVID-19, had not yet completed a 5-day course of N-R, and had not received other antiviral or monoclonal antibody treatments [6]. Time of symptom onset was reported by participants and infection was confirmed with an initial PCR or rapid antigen test. Anterior nasal swabs were self-collected about three times a week for two weeks, then weekly until persistent undetectable results. The data were originally reported relative to the time of the initial diagnostic test [6]; however, we shifted the data to be "Days post infection" (Fig 3) based on fitting the model to the data (see Data Fitting). The primary definition for viral rebound was either (a) a positive viral culture following prior negative results, or (b) nadir viral load dropping below 4 log10 copies/mL then increased by at least 1 log10 copies/mL above the nadir and sustained above 4 log10 copies/mL for two consecutive measurements [6].

For this analysis, we selected all participants who took N-R and met two criteria: (1) had at least 5 data points, with (2) at least 4 of those data points above LOD. There were 51 participants that met these criteria (20 showing rebound and 31 showing no rebound).

Details regarding the statistics of rebound in untreated individuals are presented in S4 Table in S7 Text.

Mathematical Model

We used an extension of the viral dynamic model, originally developed by Baccam et al. [75], Saenz et al. [76], and Pawelek et al. [41] to study acute influenza infections, which has previously been adapted to study SARS-CoV-2 infection dynamics [32–35]. The model below statistically outperformed the simpler versions used by Perelson et al. [27] (see S3 Table in S3 Text).

The model is described by the following set of ordinary differential equations:

$$T' = -\beta VT - \phi IT + \rho \frac{K_\rho}{I + K_\rho} R$$

$$R' = \phi IT - \rho \frac{K_\rho}{I + K_\rho} R$$

$$E' = \beta VT - kE$$

$$I' = kE - \delta(t) I$$

$$V' = \big(1 - \epsilon(C)\big)\pi I - cV$$

In this model, T is the number of target cells in the URT, E is the number of infected cells that have not yet started to produce virus, i.e., are in the eclipse phase, I is the number of productively infected cells, and V is the viral load. Target cells become infected with rate constant β. After being infected for an average time of $1/k$, infected cells in the absence of

therapy start producing virus at an adjusted rate π that accounts for sampling via a swab [33,34] and die at per capita rate δ, which we allow to be time dependent as described below. SARS-CoV-2 is cleared at per capita rate c.

For the innate immune response, we assume [34,41] the level of type-I and type-III interferons in the URT is proportional to the number of infected cells, I, because these cells produce IFN and recruit other IFN-producing cells, such as plasmacytoid dendritic cells. We also assume that interferon puts target cells in an antiviral state that is refractory to infection at rate ϕ [36–39]. The number of cells refractory to infection is denoted R. Refractory cells lose their protection and become susceptible to infection [40] at a rate $\rho \frac{K_\rho}{I+K_\rho}$. The density dependence of this rate on the number of infected cells I reflects the idea that when infected cells are abundant, they stimulate a strong interferon response, which keeps uninfected cells in a refractory state; but when infected cells decay below a critical threshold, they no longer sustain a sufficient interferon response to maintain cells in a refractory state and these cells return to being susceptible again [36–40]. Note that promoting a refractory state is just one possible mechanism of the innate immune system to fight SARS-CoV-2 infection [77]. A previous study by Ke et al. [34] examined various formulations (e.g., reduction in infection or viral production rate) that reflect different mechanisms of the innate immune response and found this formulation to be superior in capturing viral dynamics data.

We added to this model an adaptive immune response, since rebounds tend to occur late after infection, when adaptive immune responses have been observed [13]. As modeled by Pawelek et al. [41], we added this response to the model starting at time t^*. We assumed that the adaptive response increases exponentially at rate σ for the short time period we model and causes an increase in the death rate of infected cells. This increased death rate could be due to the

increasing presence of cytotoxic T cells or of viral-specific antibodies that bind to infected cells and cause their death by processes such as antibody-dependent cytotoxicity, antibody-dependent phagocytosis, or complement-mediated death. For simplicity, we fixed $\sigma = 0.5$ per day, which means that 1, 2, 3, 5 days after t^*, the adaptive immune response will be at approximately 45%, 67%, 80%, and 93% of its maximum strength. The time-dependent infected cell death rate $\delta(t)$ takes the form:

$$\delta(t) = \begin{cases} \delta_0 & \text{for } t < t^* \\ \delta_m - (\delta_m - \delta_0)e^{-\sigma(t-t^*)} & \text{for } t \geq t^* \end{cases}$$

The effectiveness of nirmatrelvir in blocking viral replication and subsequent production of virions is given by $\epsilon(C) = \epsilon_{max} \frac{C}{C+EC50}$, an E_{max} model [78] where C is the concentration of nirmatrelvir, EC_{50} is the concentration at which the drug effectiveness is half-maximal and $\epsilon_{\max}$ is the maximum effectiveness. When $\epsilon(C) = 0$ the drug has no effect and when $\epsilon(C) = 1$ the drug is 100% effective at blocking virion production. Based on the complete model, viral growth occurs only when the fraction of remaining target cells is above a critical threshold, which is $\frac{\delta(t)c}{\beta p(1-\epsilon(C))T(0)}$, corresponding to the effective reproduction number $\Re$ being larger than 1.

As it is impossible to know the number of viruses that initiated infection, we use a method suggested by Smith et al. [79] in which we assume the initiating virus is either cleared or rapidly infects cells. Thus, for initial conditions we use: $T(0) = 8 \times 10^7$ cells, $E(0) = 1$ cell, $I(0) = 0, V(0) = 0,$ and $R(0) = 0$ as explained in Ke et al. [34]. They also noted that the infection dynamics are relatively insensitive to increasing the initial number of infected cells to 10.

Pharmacokinetic and Pharmacodynamic Models for N-R

We assume the drug effectiveness $\epsilon(C)$ depends on the concentration of nirmatrelvir, $C(t)$, according to an E_{max} model with EC50 = 62 nM, as presented in the FDA Emergency Use Authorization [1]. Following a *single dose* of 300 mg nirmatrelvir with 100 mg ritonavir, the observed maximum nirmatrelvir concentration is $C_{max} = 2.21 \frac{\mu g}{mL}$ [1]. As nirmatrelvir has a molecular weight [80] of $499.54 \frac{g}{mol}$ this value of C_{max} can also be expressed as $4.4 \times 10^3\ nM$. The half-life of nirmatrelvir when taken with ritonavir is about 6 hours [1], which corresponds to an elimination rate of 2.8/day. Additionally, dosing twice-daily achieved steady-state on day 2 with approximately 2-fold accumulation [1]. Using a simple multidose absorption-elimination model, the pharmacokinetics of nirmatrelvir is given by [78]

$$C(t) = \hat{C}\frac{k_a}{k_e - k_a}\left(\frac{e^{-k_e t}}{e^{k_a I_d} - 1}\right)$$

$$\left[1 - e^{(k_e - k_a)t}(1 - e^{N_d k_a I_d}) + (e^{k_e I_d} - e^{k_a I_d})\left(\frac{e^{(N_d - 1)k_e I_d} - 1}{e^{k_e I_d} - 1}\right) - e^{((N_d - 1)k_e + k_a)I_d}\right].$$

Here, k_e is the elimination rate (2.8/day), k_a is the absorption rate (17.5/day), I_d is the dosing interval (1/2 day), $N_d = integer\left(\frac{t}{I_d}\right) + 1$ is the number of doses until time t, with the first dose at time $t = 0$. In S1 Text, we estimate $\hat{C} = \frac{FD}{V_d} = (6.25 \times 10^3$ nM). Details on the implementation of the pharmacokinetic model and the parameter values used can be found in S1 Text. With these assumptions, the drug effectiveness $\epsilon(C)$ hovers around 0.98 during treatment and then falls to zero rapidly after treatment stops (S1 Fig in S1 Text).

Data Fitting

We used a nonlinear mixed effects modeling approach (software Monolix 2023R1, Lixoft, SA, Antony, France) to fit the model to viral load data for all 51 individuals simultaneously. We applied left censoring to data points under LOD.

We assumed that the parameters p, δ_0, time of infection, and K_ρ follow a log-normal distribution. Parameters -$\log_{10}$ ϕ, -$\log_{10}$ β, ρ, and t^* were assumed to follow a logit-normal distribution, with ranges closely following literature values [33,34]. We constrained $-\log_{10}\beta$ between 7.5 and 9. Parameter ρ was constrained between 0 and 1 per day, $-\log_{10}\phi$ between 5 and 12, and t^* between 7 and 28 days. No covariate was used during the initial fitting. A covariate based on whether a participant is classified as rebound or non-rebound was used later with the best fit model to determine the parameters that are different between these two groups.

The viral load data was originally reported relative to the number days since the initial PCR confirmation test. To estimate the time of infection, we shifted the data to be relative to the reported time of symptom onset. We then estimated the interval from the time of infection, or more precisely the time interval from when virus begins to grow exponentially as estimated by our model fitting, to when the participant reported symptoms. We then shifted the viral load data to be relative to this estimated time of infection.

The process to optimize the initial guesses of fitting parameters was done manually within the given parameter ranges to avoid unrealistic model dynamics. Whenever two models share a fitting parameter, the same initial guess for that parameter would be used in the fitting of both models. Model comparisons were done using the corrected Bayesian Information Criterion (BICc) [81] as reported by Monolix.

Construction of an In-Silico Cohort

To quantify the chance of viral rebound after a five-day (or longer) course of treatment with N-R, we simulated a cohort of *in silico* patients. We used the following selection criteria to construct the cohort of *in silico* patients with typical viral load patterns: (1) The viral load must peak above 10^6 copies per mL; (2) The peak must be reached between day 2 and day 7 after infection; (3) The viral load must decline below 10^2 copies per mL by day 28. This algorithm is akin to a rejection algorithm, where we sample each parameter from the best fit population estimates (i.e., the estimated distribution) and only accept parameter sets that satisfy conditions (1) – (3). We fixed the time the adaptive immune response starts, t^*, to the population estimate of 13 days, and set δ_m = 20/day to prevent unrealistic rebound once an effective immune response has been developed. Additional details of the *in silico* cohort are presented in S8 Text.

We used these admissible parameter sets to simulate treatment of different durations (5-, 6-, 7-, 8-, and 10-day of N-R) starting at different times (1 to 4 days post symptom onset) and calculate the probability of rebound. We also examined how a potential delay in the development of the adaptive immune response with longer treatment may affect the likelihood of rebound (S9 Text).

Acknowledgements

The authors thank Jeremie Guedj for helpful comments on the manuscript.

References

[1] FACT SHEET FOR HEALTHCARE PROVIDERS: EMERGENCY USE AUTHORIZATION FOR PAXLOVID 2023.

[2] Hammond J, Leister-Tebbe H, Gardner A, Abreu P, Bao W, Wisemandle W, et al. Oral Nirmatrelvir for High-Risk, Nonhospitalized Adults with Covid-19. N Engl J Med 2022;386:1397–408. https://doi.org/10.1056/NEJMoa2118542.

[3] Arbel R, Wolff Sagy Y, Hoshen M, Battat E, Lavie G, Sergienko R, et al. Nirmatrelvir Use and Severe Covid-19 Outcomes during the Omicron Surge. N Engl J Med 2022;387:790–8. https://doi.org/10.1056/NEJMoa2204919.

[4] Wong CKH, Au ICH, Lau KTK, Lau EHY, Cowling BJ, Leung GM. Real-world effectiveness of molnupiravir and nirmatrelvir plus ritonavir against mortality, hospitalisation, and in-hospital outcomes among community-dwelling, ambulatory patients with confirmed SARS-CoV-2 infection during the omicron wave in Hong Kong: an observational study. The Lancet 2022;400:1213–22. https://doi.org/10.1016/S0140-6736(22)01586-0.

[5] Charness ME, Gupta K, Stack G, Strymish J, Adams E, Lindy DC, et al. Rebound of SARS-CoV-2 Infection after Nirmatrelvir–Ritonavir Treatment. N Engl J Med 2022;387:1045–7. https://doi.org/10.1056/NEJMc2206449.

[6] Edelstein GE, Boucau J, Uddin R, Marino C, Liew MY, Barry M, et al. SARS-CoV-2 Virologic Rebound With Nirmatrelvir–Ritonavir Therapy: An Observational Study. Ann Intern Med 2023;176:1577–85. https://doi.org/10.7326/M23-1756.

[7] Boucau J, Uddin R, Marino C, Regan J, Flynn JP, Choudhary MC, et al. Characterization of Virologic Rebound Following Nirmatrelvir-Ritonavir Treatment for Coronavirus Disease 2019 (COVID-19). Clin Infect Dis 2023;76:e526–9. https://doi.org/10.1093/cid/ciac512.

[8] Duan Y, Zhou H, Liu X, Iketani S, Lin M, Zhang X, et al. Molecular mechanisms of SARS-CoV-2 resistance to nirmatrelvir. Nature 2023;622:376–82. https://doi.org/10.1038/s41586-023-06609-0.

[9] Iketani S, Mohri H, Culbertson B, Hong SJ, Duan Y, Luck MI, et al. Multiple pathways for SARS-CoV-2 resistance to nirmatrelvir. Nature 2023;613:558–64. https://doi.org/10.1038/s41586-022-05514-2.

[10] Tamura TJ, Choudhary MC, Deo R, Yousuf F, Gomez AN, Edelstein GE, et al. Emerging SARS-CoV-2 Resistance after Antiviral Treatment. JAMA Netw Open 2024;(In Press).

[11] Soares H, Baniecki ML, Cardin R, Leister-Tebbe H, Zhu Y, Guan S, et al. Viral Load Rebound in Placebo and Nirmatrelvir-Ritonavir Treated COVID-19 Patients is not Associated with Recurrence of Severe Disease or Mutations. In Review; 2022. https://doi.org/10.21203/rs.3.rs-1720472/v2.

[12] Carlin AF, Clark AE, Chaillon A, Garretson AF, Bray W, Porrachia M, et al. Virologic and Immunologic Characterization of Coronavirus Disease 2019 Recrudescence After Nirmatrelvir/Ritonavir Treatment. Clin Infect Dis 2023;76:e530–2. https://doi.org/10.1093/cid/ciac496.

[13] Epling BP, Rocco JM, Boswell KL, Laidlaw E, Galindo F, Kellogg A, et al. Clinical, Virologic, and Immunologic Evaluation of Symptomatic Coronavirus Disease 2019 Rebound Following Nirmatrelvir/Ritonavir Treatment. Clin Infect Dis 2023;76:573–81. https://doi.org/10.1093/cid/ciac663.

[14] Tamura TJ. Analysis of emergent SARS-CoV-2 antiviral resistance and its association with virological rebound 2024.

[15] Zuckerman NS, Bucris E, Keidar-Friedman D, Amsalem M, Brosh-Nissimov T. Nirmatrelvir Resistance—de Novo E166V/L50V Mutations in an Immunocompromised Patient Treated With Prolonged Nirmatrelvir/Ritonavir Monotherapy Leading to Clinical and Virological Treatment Failure—a Case Report. Clin Infect Dis 2024;78:352–5. https://doi.org/10.1093/cid/ciad494.

[16] Hirotsu Y, Kobayashi H, Kakizaki Y, Saito A, Tsutsui T, Kawaguchi M, et al. Multidrug-resistant mutations to antiviral and antibody therapy in an immunocompromised patient infected with SARS-CoV-2. Med 2023;4:813-824.e4. https://doi.org/10.1016/j.medj.2023.08.001.

[17] Anderson AS, Caubel P, Rusnak JM. Nirmatrelvir–Ritonavir and Viral Load Rebound in Covid-19. N Engl J Med 2022;387:1047–9. https://doi.org/10.1056/NEJMc2205944.

[18] Ranganath N, O'Horo JC, Challener DW, Tulledge-Scheitel SM, Pike ML, O'Brien M, et al. Rebound Phenomenon After Nirmatrelvir/Ritonavir Treatment of Coronavirus Disease 2019 (COVID-19) in High-Risk Persons. Clin Infect Dis 2023;76:e537–9. https://doi.org/10.1093/cid/ciac481.

[19] Dai EY, Lee KA, Nathanson AB, Leonelli AT, Petros BA, Brock-Fisher T, et al. Viral Kinetics of Severe Acute Respiratory Syndrome Coronavirus 2 (SARS-CoV-2) Omicron Infection in mRNA-Vaccinated

572 Individuals Treated and Not Treated with Nirmatrelvir-Ritonavir. Infectious Diseases (except HIV/AIDS);
573 2022. https://doi.org/10.1101/2022.08.04.22278378.
574 [20] Wong CKH, Lau KTK, Au ICH, Lau EHY, Poon LLM, Hung IFN, et al. Viral burden rebound in hospitalised
575 patients with COVID-19 receiving oral antivirals in Hong Kong: a population-wide retrospective cohort study.
576 Lancet Infect Dis 2023;23:683–95. https://doi.org/10.1016/S1473-3099(22)00873-8.
577 [21] Wang L, Berger NA, Davis PB, Kaelber DC, Volkow ND, Xu R. COVID-19 rebound after Paxlovid and
578 Molnupiravir during January-June 2022. Infectious Diseases (except HIV/AIDS); 2022.
579 https://doi.org/10.1101/2022.06.21.22276724.
580 [22] Smith-Jeffcoat SE, Biddle JE, Talbot HK, Morrissey KG, Stockwell MS, Maldonado Y, et al. Symptoms,
581 Viral Loads, and Rebound Among COVID-19 Outpatients Treated With Nirmatrelvir/Ritonavir Compared
582 With Propensity Score–Matched Untreated Individuals. Clin Infect Dis 2024;78:1175–84.
583 https://doi.org/10.1093/cid/ciad696.
584 [23] Hay JA, Kissler SM, Fauver JR, Mack C, Tai CG, Samant RM, et al. Quantifying the impact of immune
585 history and variant on SARS-CoV-2 viral kinetics and infection rebound: A retrospective cohort study. eLife
586 2022;11:e81849. https://doi.org/10.7554/eLife.81849.
587 [24] Deo R, Choudhary MC, Moser C, Ritz J, Daar ES, Wohl DA, et al. Symptom and Viral Rebound in Untreated
588 SARS-CoV-2 Infection. Ann Intern Med 2023;176:348–54. https://doi.org/10.7326/M22-2381.
589 [25] Pandit JA, Radin JM, Chiang DC, Spencer EG, Pawelek JB, Diwan M, et al. The Coronavirus Disease 2019
590 Rebound Study: A Prospective Cohort Study to Evaluate Viral and Symptom Rebound Differences in
591 Participants Treated With Nirmatrelvir Plus Ritonavir Versus Untreated Controls. Clin Infect Dis 2023;77:25–
592 31. https://doi.org/10.1093/cid/ciad102.
593 [26] Wong GL-H, Yip TC-F, Lai MS-M, Wong VW-S, Hui DS-C, Lui GC-Y. Incidence of Viral Rebound After
594 Treatment With Nirmatrelvir-Ritonavir and Molnupiravir. JAMA Netw Open 2022;5:e2245086.
595 https://doi.org/10.1001/jamanetworkopen.2022.45086.
596 [27] Perelson AS, Ribeiro RM, Phan T. An explanation for SARS-CoV-2 rebound after Paxlovid treatment.
597 Infectious Diseases (except HIV/AIDS); 2023. https://doi.org/10.1101/2023.05.30.23290747.
598 [28] Cao B, Wang Y, Lu H, Huang C, Yang Y, Shang L, et al. Oral Simnotrelvir for Adult Patients with Mild-to-
599 Moderate Covid-19. N Engl J Med 2024;390:230–41. https://doi.org/10.1056/NEJMoa2301425.
600 [29] Yang X-M, Yang Y, Yao B-F, Ye P-P, Xu Y, Peng S-P, et al. A first-in-human phase 1 study of simnotrelvir,
601 a 3CL-like protease inhibitor for treatment of COVID-19, in healthy adult subjects. Eur J Pharm Sci
602 2023;191:106598. https://doi.org/10.1016/j.ejps.2023.106598.
603 [30] Yang Z, Xu Y, Zheng R, Ye L, Lv G, Cao Z, et al. COVID-19 Rebound After VV116 vs Nirmatrelvir-
604 Ritonavir Treatment: A Randomized Clinical Trial. JAMA Netw Open 2024;7:e241765.
605 https://doi.org/10.1001/jamanetworkopen.2024.1765.
606 [31] Cao Z, Gao W, Bao H, Feng H, Mei S, Chen P, et al. VV116 versus Nirmatrelvir–Ritonavir for Oral
607 Treatment of Covid-19. N Engl J Med 2023;388:406–17. https://doi.org/10.1056/NEJMoa2208822.
608 [32] Phan T, Zitzmann C, Chew KW, Smith DM, Daar ES, Wohl DA, et al. Modeling the emergence of viral
609 resistance for SARS-CoV-2 during treatment with an anti-spike monoclonal antibody. PLOS Pathog
610 2024;20:e1011680. https://doi.org/10.1371/journal.ppat.1011680.
611 [33] Ke R, Martinez PP, Smith RL, Gibson LL, Mirza A, Conte M, et al. Daily longitudinal sampling of SARS-
612 CoV-2 infection reveals substantial heterogeneity in infectiousness. Nat Microbiol 2022;7:640–52.
613 https://doi.org/10.1038/s41564-022-01105-z.
614 [34] Ke R, Zitzmann C, Ho DD, Ribeiro RM, Perelson AS. In vivo kinetics of SARS-CoV-2 infection and its
615 relationship with a person's infectiousness. Proc Natl Acad Sci 2021;118:e2111477118.
616 https://doi.org/10.1073/pnas.2111477118.
617 [35] Owens K, Esmaeili S, Schiffer JT. Heterogeneous SARS-CoV-2 kinetics due to variable timing and intensity
618 of immune responses. JCI Insight 2024;9:e176286. https://doi.org/10.1172/jci.insight.176286.
619 [36] Samuel CE. Antiviral Actions of Interferons. Clin Microbiol Rev 2001;14:778–809.
620 https://doi.org/10.1128/CMR.14.4.778-809.2001.
621 [37] Talemi SR, Höfer T. Antiviral interferon response at single-cell resolution. Immunol Rev 2018;285:72–80.
622 https://doi.org/10.1111/imr.12699.
623 [38] Voigt EA, Swick A, Yin J. Rapid induction and persistence of paracrine-induced cellular antiviral states arrest
624 viral infection spread in A549 cells. Virology 2016;496:59–66. https://doi.org/10.1016/j.virol.2016.05.019.
625 [39] García-Sastre A, Biron CA. Type 1 Interferons and the Virus-Host Relationship: A Lesson in Détente. Science
626 2006;312:879–82. https://doi.org/10.1126/science.1125676.

[40] Samuel CE, Knutson GS. Mechanism of interferon action. Kinetics of decay of the antiviral state and protein phosphorylation in mouse fibroblasts treated with natural and cloned interferons. J Biol Chem 1982;257:11796–801. https://doi.org/10.1016/S0021-9258(18)33834-1.

[41] Pawelek KA, Huynh GT, Quinlivan M, Cullinane A, Rong L, Perelson AS. Modeling Within-Host Dynamics of Influenza Virus Infection Including Immune Responses. PLoS Comput Biol 2012;8:e1002588. https://doi.org/10.1371/journal.pcbi.1002588.

[42] De Boer RJ, Oprea M, Antia R, Murali-Krishna K, Ahmed R, Perelson AS. Recruitment Times, Proliferation, and Apoptosis Rates during the CD8 $^{+}$ T-Cell Response to Lymphocytic Choriomeningitis Virus. J Virol 2001;75:10663–9. https://doi.org/10.1128/JVI.75.22.10663-10669.2001.

[43] Esmaeili S, Owens K, Wagoner J, Polyak SJ, White JM, Schiffer JT. A unifying model to explain frequent SARS-CoV-2 rebound after nirmatrelvir treatment and limited prophylactic efficacy. Nat Commun 2024;15:5478. https://doi.org/10.1038/s41467-024-49458-9.

[44] Wong CKH, Lau JJ, Au ICH, Lau KTK, Hung IFN, Peiris M, et al. Optimal timing of nirmatrelvir/ritonavir treatment after COVID-19 symptom onset or diagnosis: target trial emulation. Nat Commun 2023;14:8377. https://doi.org/10.1038/s41467-023-43706-0.

[45] Cohen MS, Brown ER. Rebound of COVID-19 With Nirmatrelvir–Ritonavir Antiviral Therapy. Ann Intern Med 2023;176:1672–3. https://doi.org/10.7326/M23-2887.

[46] Chiarelli A, Dobrovolny H. Viral Rebound After Antiviral Treatment: A Mathematical Modeling Study of the Role of Antiviral Mechanism of Action. Interdiscip Sci Comput Life Sci 2024. https://doi.org/10.1007/s12539-024-00643-w.

[47] Frediani JK, Parsons R, McLendon KB, Westbrook AL, Lam W, Martin G, et al. The New Normal: Delayed Peak Severe Acute Respiratory Syndrome Coronavirus 2 (SARS-CoV-2) Viral Loads Relative to Symptom Onset and Implications for Coronavirus Disease 2019 (COVID-19) Testing Programs. Clin Infect Dis 2023:ciad582. https://doi.org/10.1093/cid/ciad582.

[48] Yang Y, Guo L, Yuan J, Xu Z, Gu Y, Zhang J, et al. Viral and antibody dynamics of acute infection with SARS-CoV-2 omicron variant (B.1.1.529): a prospective cohort study from Shenzhen, China. Lancet Microbe 2023;4:e632–41. https://doi.org/10.1016/S2666-5247(23)00139-8.

[49] Zhou K, Hu B, Zhao X, Chi H, Pan J, Zheng Y, et al. Longitudinal observation of viral load in patients infected with Omicron variant and its relationship with clinical symptoms. Front Microbiol 2023;13:1037733. https://doi.org/10.3389/fmicb.2022.1037733.

[50] Du Z, Wang L, Bai Y, Liu Y, Lau EH, Galvani AP, et al. A retrospective cohort study of Paxlovid efficacy depending on treatment time in hospitalized COVID-19 patients. eLife 2024;13:e89801. https://doi.org/10.7554/eLife.89801.

[51] Wang Y, Chen X, Xiao W, Zhao D, Feng L. Rapid COVID-19 rebound in a severe COVID-19 patient during 20-day course of Paxlovid. J Infect 2022;85:e134–6. https://doi.org/10.1016/j.jinf.2022.08.012.

[52] COVID-19 Rebound After Paxlovid Treatment 2022.

[53] Fumagalli V, Di Lucia P, Ravà M, Marotta D, Bono E, Grassi S, et al. Nirmatrelvir treatment of SARS-CoV-2-infected mice blunts antiviral adaptive immune responses. EMBO Mol Med 2023;15:e17580. https://doi.org/10.15252/emmm.202317580.

[54] Carlin AF, Clark AE, Garretson AF, Bray W, Porrachia M, Santos AT, et al. Neutralizing Antibody Responses After Severe Acute Respiratory Syndrome Coronavirus 2 BA.2 and BA.2.12.1 Infection Do Not Neutralize BA.4 and BA.5 and Can Be Blunted by Nirmatrelvir/Ritonavir Treatment. Open Forum Infect Dis 2023;10:ofad154. https://doi.org/10.1093/ofid/ofad154.

[55] Weinstein E. Extended Nirmatrelvir/Ritonavir Treatment Durations for Immunocompromised Patients with COVID-19 (Poster 00658) 2024.

[56] Nair MS, Luck MI, Huang Y, Sabo Y, Ho DD. Persistence of an Infectious Form of SARS-CoV-2 After Protease Inhibitor Treatment of Permissive Cells In Vitro. J Infect Dis 2024:jiae385. https://doi.org/10.1093/infdis/jiae385.

[57] Yotsuyanagi H, Ohmagari N, Doi Y, Yamato M, Bac NH, Cha BK, et al. Efficacy and Safety of 5-Day Oral Ensitrelvir for Patients With Mild to Moderate COVID-19: The SCORPIO-SR Randomized Clinical Trial. JAMA Netw Open 2024;7:e2354991. https://doi.org/10.1001/jamanetworkopen.2023.54991.

[58] Shimizu R, Sonoyama T, Fukuhara T, Kuwata A, Matsuo Y, Kubota R. Safety, Tolerability, and Pharmacokinetics of the Novel Antiviral Agent Ensitrelvir Fumaric Acid, a SARS-CoV-2 3CL Protease Inhibitor, in Healthy Adults. Antimicrob Agents Chemother 2022;66:e00632-22. https://doi.org/10.1128/aac.00632-22.

682 [59] Vellas C, Kamar N, Izopet J. Resistance mutations in SARS-CoV-2 omicron variant after tixagevimab-
683 cilgavimab treatment. J Infect 2022;85:e162–3. https://doi.org/10.1016/j.jinf.2022.07.014.
684 [60] Vellas C, Trémeaux P, Del Bello A, Latour J, Jeanne N, Ranger N, et al. Resistance mutations in SARS-CoV-
685 2 omicron variant in patients treated with sotrovimab. Clin Microbiol Infect 2022;28:1297–9.
686 https://doi.org/10.1016/j.cmi.2022.05.002.
687 [61] Jensen B, Luebke N, Feldt T, Keitel V, Brandenburger T, Kindgen-Milles D, et al. Emergence of the E484K
688 mutation in SARS-COV-2-infected immunocompromised patients treated with bamlanivimab in Germany.
689 Lancet Reg Health - Eur 2021;8:100164. https://doi.org/10.1016/j.lanepe.2021.100164.
690 [62] Choudhary MC, Chew KW, Deo R, Flynn JP, Regan J, Crain CR, et al. Emergence of SARS-CoV-2 escape
691 mutations during Bamlanivimab therapy in a phase II randomized clinical trial. Nat Microbiol 2022;7:1906–
692 17. https://doi.org/10.1038/s41564-022-01254-1.
693 [63] Peiffer-Smadja N, Bridier-Nahmias A, Ferré VM, Charpentier C, Garé M, Rioux C, et al. Emergence of
694 E484K Mutation Following Bamlanivimab Monotherapy among High-Risk Patients Infected with the Alpha
695 Variant of SARS-CoV-2. Viruses 2021;13:1642. https://doi.org/10.3390/v13081642.
696 [64] Liberti DC, Kremp MM, Liberti WA, Penkala IJ, Li S, Zhou S, et al. Alveolar epithelial cell fate is maintained
697 in a spatially restricted manner to promote lung regeneration after acute injury. Cell Rep 2021;35:109092.
698 https://doi.org/10.1016/j.celrep.2021.109092.
699 [65] Bridges JP, Vladar EK, Huang H, Mason RJ. Respiratory epithelial cell responses to SARS-CoV-2 in
700 COVID-19. Thorax 2022;77:203–9. https://doi.org/10.1136/thoraxjnl-2021-217561.
701 [66] Fang Y, Liu H, Huang H, Li H, Saqi A, Qiang L, et al. Distinct stem/progenitor cells proliferate to regenerate
702 the trachea, intrapulmonary airways and alveoli in COVID-19 patients. Cell Res 2020;30:705–7.
703 https://doi.org/10.1038/s41422-020-0367-9.
704 [67] Killingley B, Mann AJ, Kalinova M, Boyers A, Goonawardane N, Zhou J, et al. Safety, tolerability and viral
705 kinetics during SARS-CoV-2 human challenge in young adults. Nat Med 2022;28:1031–41.
706 https://doi.org/10.1038/s41591-022-01780-9.
707 [68] Gunawardana M, Webster S, Rivera S, Cortez JM, Breslin J, Pinales C, et al. Early SARS-CoV-2 dynamics
708 and immune responses in unvaccinated participants of an intensely sampled longitudinal surveillance study.
709 Commun Med 2022;2:129. https://doi.org/10.1038/s43856-022-00195-4.
710 [69] Zitzmann C, Ke R, Ribeiro RM, Perelson AS. How robust are estimates of key parameters in standard viral
711 dynamic models? PLOS Comput Biol 2024;20:e1011437. https://doi.org/10.1371/journal.pcbi.1011437.
712 [70] Ciupe SM, Tuncer N. Identifiability of parameters in mathematical models of SARS-CoV-2 infections in
713 humans. Sci Rep 2022;12:14637. https://doi.org/10.1038/s41598-022-18683-x.
714 [71] Kissler SM, Fauver JR, Mack C, Tai CG, Breban MI, Watkins AE, et al. Viral Dynamics of SARS-CoV-2
715 Variants in Vaccinated and Unvaccinated Persons. N Engl J Med 2021;385:2489–91.
716 https://doi.org/10.1056/NEJMc2102507.
717 [72] Puhach O, Meyer B, Eckerle I. SARS-CoV-2 viral load and shedding kinetics. Nat Rev Microbiol 2022.
718 https://doi.org/10.1038/s41579-022-00822-w.
719 [73] Wagstaffe HR, Thwaites RS, Reynaldi A, Sidhu JK, McKendry R, Ascough S, et al. Mucosal and systemic
720 immune correlates of viral control after SARS-CoV-2 infection challenge in seronegative adults. Sci Immunol
721 2024;9:eadj9285. https://doi.org/10.1126/sciimmunol.adj9285.
722 [74] Boucau J, Marino C, Regan J, Uddin R, Choudhary MC, Flynn JP, et al. Duration of Shedding of Culturable
723 Virus in SARS-CoV-2 Omicron (BA.1) Infection. N Engl J Med 2022;387:275–7.
724 https://doi.org/10.1056/NEJMc2202092.
725 [75] Baccam P, Beauchemin C, Macken CA, Hayden FG, Perelson AS. Kinetics of Influenza A Virus Infection in
726 Humans. J Virol 2006;80:7590–9. https://doi.org/10.1128/JVI.01623-05.
727 [76] Saenz RA, Quinlivan M, Elton D, MacRae S, Blunden AS, Mumford JA, et al. Dynamics of Influenza Virus
728 Infection and Pathology. J Virol 2010;84:3974–83. https://doi.org/10.1128/JVI.02078-09.
729 [77] Diamond MS, Lambris JD, Ting JP, Tsang JS. Considering innate immune responses in SARS-CoV-2
730 infection and COVID-19. Nat Rev Immunol 2022;22:465–70. https://doi.org/10.1038/s41577-022-00744-x.
731 [78] Dixit NM, Perelson AS. Complex patterns of viral load decay under antiretroviral therapy: influence of
732 pharmacokinetics and intracellular delay. J Theor Biol 2004;226:95–109.
733 https://doi.org/10.1016/j.jtbi.2003.09.002.
734 [79] Smith AP, Moquin DJ, Bernhauerova V, Smith AM. Influenza Virus Infection Model With Density
735 Dependence Supports Biphasic Viral Decay. Front Microbiol 2018;9:1554.
736 https://doi.org/10.3389/fmicb.2018.01554.

[80] PubChem. Nirmatrelvir n.d. https://pubchem.ncbi.nlm.nih.gov/compound/155903259 (accessed March 7, 2024).

[81] Burnham KP, Anderson DR. Practical Use of the Information-Theoretic Approach. Model Sel. Inference, New York, NY: Springer New York; 1998, p. 75–117. https://doi.org/10.1007/978-1-4757-2917-7_3.

Funding: This work was performed under the auspices of the US Dept. of Energy under contract 89233218CNA000001 and supported by

National Institutes of Health grant U54-HL143541-04 (RMR)

Los Alamos National Laboratory LDRD 20200743ER (RMR), 20200695ER (ASP), 20210730ER (RMR), and 20220791PRD2 (TP).

Massachusetts Consortium on Pathogen Readiness (JZL, JEL, AKB, MJS)

Massachusetts General Hospital Department of Medicine (JMV, AKB, MJS)

National Institutes of Health grant U19 AI110818 (JZL, JEL, AKB, MJS)

National Institutes of Health grant R01 AI176287 (JZL, JEL, AKB, MJS)

Author contributions

Conceptualization: ASP, RMR, TP, JZL, MJS, AKB, JEL

Data curation: GEE, JB, RU, CM, MYL, MB, MCC, DT, KS, ZR, YL, SS, TDV, YK, JAS, SPH, ZW, JMV, JZL, MJS, AKB, JEL

Methodology: ASP, RMR, TP

Investigation: ASP, RMR, TP, JZL, MJS, AKB, JEL

Visualization: TP

Funding acquisition: ASP, RMR, TP, JMV, JZL, MJS, AKB, JEL

Project administration: ASP, RMR, JZL, MJS, AKB, JEL

Supervision: ASP, RMR, JZL, MJS, AKB, JEL

Writing – original draft: TP

Writing – review & editing: ASP, RMR, TP, GEE, JB, RU, CM, MYL, MB, MCC, DT, KS, ZR, YL, SS, TDV, YK, JAS, SPH, ZW, JMV, JZL, MJS, AKB, JEL

Competing interests: ASP owns stock in Pfizer. He was also on a Pfizer advisory committee and received an honorarium. The other authors declare that they have no competing interests.

Data and materials availability: The de-identified viral load data is provided in supplementary material (SM Data). Codes for fitting, plotting, and *in silico* analyses will be made available on GitHub once the manuscript is accepted and before its publication.

Supplementary Materials

S1 to S10 Text

S1 to S9 Figs

S1 to S4 Tables